



Article

Pancancer Analysis of the Oncogenic and Prognostic Role of *NOL7*: A Potential Target for Carcinogenesis and Survival

Qiaojun Liu ^{1,2}, Renjian Xie ^{2,3,4}  and Yumei Li ^{1,2,3,*}

¹ School of Basic Medicine, Gannan Medical University, Ganzhou 341000, China

² Key Laboratory of Biomaterials and Biofabrication in Tissue Engineering of Jiangxi Province, Ganzhou 341000, China

³ Key Laboratory of Prevention and Treatment of Cardiovascular and Cerebrovascular Diseases, Ministry of Education, Gannan Medical University, Ganzhou 341000, China

⁴ School of Medical Information Engineering, Gannan Medical University, Ganzhou 341000, China

* Correspondence: yumei.li@gmu.edu.cn

Abstract: Despite growing evidence suggesting the critical function of *NOL7* in cancer initiation and development, a systematic pancancer analysis of *NOL7* is lacking. Herein, we present a comprehensive study of *NOL7* which aimed to explore its potential role and detailed mechanisms across 33 human tumors based on The Cancer Genome Atlas (TCGA) and Clinical Proteomic Tumor Analysis Consortium (CATPAC) databases. As a result, both gene and protein levels of *NOL7* were found to be increased in various tumor tissues, including breast invasive carcinoma (BRCA), colon adenocarcinoma (COAD), hepatocellular carcinoma (LIHC), lung adenocarcinoma (LUAD), and head and neck squamous cell carcinoma (HNSC) as compared with corresponding normal tissues. Meanwhile, dysregulated *NOL7* expression was found to be closely related to pathological stage and prognosis in several cancers, including LIHC, ovarian serous cystadenocarcinoma (OV), and bladder urothelial carcinoma (BLCA). The DNA methylation level of *NOL7* was found to be decreased in most cancers and to be negatively associated with *NOL7* expression. Furthermore, *NOL7* expression was determined to be significantly associated with levels of infiltrating cells and immune checkpoint genes, including *HMGB1*. Analysis of *NOL7*-related genes revealed that RNA metabolism pathways, including “ribosome biogenesis”, “spliceosome”, and “RNA transport”, were mainly involved in the functional mechanism of *NOL7* in human cancers. In summary, this pancancer study characterized the relationship between *NOL7* expression and clinicopathologic features in multiple cancer types and further showed its potential regulatory network in human cancers. It represents a systemic analysis for further functional and therapeutic studies of *NOL7* and highlights its predictive value with respect to the carcinogenesis and prognosis of various cancers, especially LIHC.

Keywords: *NOL7*; pancancer; oncogenesis; prognosis; human tumor; enrichment analysis; big data



Citation: Liu, Q.; Xie, R.; Li, Y. Pancancer Analysis of the Oncogenic and Prognostic Role of *NOL7*: A Potential Target for Carcinogenesis and Survival. *Int. J. Mol. Sci.* **2022**, *23*, 9611. <https://doi.org/10.3390/ijms23179611>

Academic Editor: Alvaro Galli

Received: 24 July 2022

Accepted: 23 August 2022

Published: 25 August 2022

Publisher's Note: MDPI stays neutral with regard to jurisdictional claims in published maps and institutional affiliations.



Copyright: © 2022 by the authors. Licensee MDPI, Basel, Switzerland. This article is an open access article distributed under the terms and conditions of the Creative Commons Attribution (CC BY) license (<https://creativecommons.org/licenses/by/4.0/>).

1. Introduction

Targeted therapy has become mainstream and one of the most effective strategies for cancer treatment [1]. However, the curability and prognosis of patients remain unsatisfactory due to an insufficiency of targeted drugs. The therapeutic effects of current targeted drugs are also limited by the emergence of drug resistance [2]. Therefore, it is necessary to explore novel and unique therapeutic targets for cancer treatment. Pancancer analysis represents a systemic approach to the characterization of genes of interest in multiple cancers. It is a promising method for investigating the relationship between genes or molecules and potential related theories of carcinogenesis as well as cancer progression. It can also provide a theoretical reference for the development of new tumor-targeting drugs and further expansion of the population who may benefit from targeted therapy [3].

The human *NOL7* gene is located at 6p23, a chromosomal region frequently lost in several malignancies, including cervical cancer [4]. It was first reported in 2006 by Lingen

MW et al. that *NOL7* serves as a tumor suppressor gene in cervical cancer [5]. Both loss of heterozygosity and decreased mRNA/protein expression of *NOL7* were observed in cervical cancer, and it was found to be downregulated with disease progression. Meanwhile, *NOL7* can predict cancer recurrence and survival in cervical cancer patients. Researchers found that tumor-associated mutations and SNP variations harbored in the *NOL7* gene potentially contribute to the loss of *NOL7* in cancer cells [6,7]. In addition, C-myc and RXR α transcription factors were found to positively regulate *NOL7* expression [4]. MW Lingen et al. also revealed that transcription of *NOL7* was positively regulated by the *RB* tumor suppressor in cervical cancer and that it further functioned as an mRNA-binding protein to modulate TSP-1 expression by enhancing the post-transcriptional stability of its mRNA, thus inducing an anti-angiogenic and tumor-suppressive phenotype [8,9]. The *NOL7* gene encodes nucleolar protein 7, which has three alternatively spliced forms, each isoform differently localized within the cell. *NOL7*-SP1 (29 kD) is predominantly localized in the cell nucleolus, with some nucleoplasmic distribution; *NOL7*-SP2 (16 kD) is nucleoplasmic and has a moderate nucleolar distribution; while *NOL7*-SP3 (12 kD) is mostly distributed in the nucleoplasm, with some cytoplasmic distribution. A strong nuclear localization signal within the C-terminus of *NOL7*-SP1 contributes to its translocation into the cell nucleus. Nucleolus-localized *NOL7* protein is typically involved in maintaining internal nucleolar structure and cell growth, whereas nucleoplasm-localized *NOL7* protein exerts anti-angiogenic effects [10,11]. It is well worth noting that the chromosome region 6p23, where the *NOL7* gene resides, frequently undergoes heterozygous loss in cervical cancer, and this region is commonly associated with the amplification of melanoma [12]. Thus, our previous research determined that *NOL7* was upregulated in melanoma development and exhibited tumor-promoting activity [13]. The multifaceted function of *NOL7* suggested that its investigation might enable mechanistic insights into the potential role of *NOL7* in malignancy. However, a systematic assessment of *NOL7* in human cancer remains unavailable.

Given the critical role of *NOL7* in cancer, we first combined TCGA project, GTEx, and CPTAC datasets to conduct a pancancer analysis of *NOL7* in various human cancers. This comprehensive study aimed to clarify the potential function and regulatory mechanisms of *NOL7* in the pathogenesis or clinical prognosis of multiple cancer types and further confirm its promising role as a diagnostic biomarker and therapeutic target for cancer treatment.

2. Results

2.1. Pancancer Analysis of *NOL7* Expression

As shown in Supplementary Figure S1a, the *NOL7* gene is localized at the 6p23 chromosomal region (chromosome 6: 13,615,335–13,632,739 forward strand). We downloaded data on the subcellular localization and tissue localization of the *NOL7* protein from the HPA database and found that the *NOL7* protein had the highest expression in the kidneys, followed by the pancreas (Supplementary Figure S1b–c). Overall, *NOL7* showed low RNA specificity in tissue as well as in blood cells (Supplementary Figure S1d–e).

Moreover, a gene expression landscape of *NOL7* across human cancers was constructed based on TCGA project data. Figure 1a shows significant differences in the transcriptional levels of *NOL7* between tumor tissues versus adjacent normal tissues in 16 types of cancer. Compared with normal tissue, increased *NOL7* expression was observed in BLCA, BRCA, cholangiocarcinoma (CHOL), COAD, esophageal carcinoma (ESCA), head and neck squamous cell carcinoma (HNSC), LIHC, LUAD, lung squamous cell carcinoma (LUSC), prostate adenocarcinoma (PRAD), and stomach adenocarcinoma (STAD) (all *p*-values < 0.001). Conversely, decreased *NOL7* expression was detected in kidney chromophobe (KICH), kidney renal clear cell carcinoma (KIRC), kidney renal papillary cell carcinoma (KIRP), and thyroid carcinoma (THCA) tissues (all *p*-values < 0.001) as compared with normal tissues. We also incorporated the GTEx datasets to supplement the number of normal tissues included as controls in the TCGA project. As shown in Figure 1b, *NOL7* levels were significantly higher in thymoma (THYM), CHOL, DLBC, LIHC, and pancreatic

In addition, we utilized CPTAC datasets to detect the differences in *NOL7* protein levels between tumor tissues and corresponding normal tissues. The protein levels of *NOL7* were found to be notably increased in breast cancer, ovarian cancer, colon cancer, hepatocellular carcinoma, KIRC, adrenocortical carcinoma (RCC), LUAD, glioblastoma multiforme (GBM), and HNSC tissues (all p -values < 0.001) but decreased in PAAD tissues ($p < 0.05$) as compared with relevant healthy tissues (Figure 1c). The immunohistochemistry staining images of *NOL7* proteins in various tumors and corresponding normal tissues are shown in Supplementary Figure S2.

2.2. Pancancer Analysis of the Relationship between *NOL7* Expression and Clinicopathology

To investigate the association between *NOL7* and clinicopathological features, we analyzed the expression patterns of *NOL7* in normal tissues and stages I, II, III and IV tumor tissues in multiple cancers using the UALCAN tool. As shown in Figure 2, *NOL7* expression was confirmed to be significantly upregulated during disease progression from normal tissue to early malignancy and further to the terminal stage in cancers, including BLCA, BRCA, CHOL, COAD, ESCA, HNSC, LIHC, LUAD, LUSC, READ, and STAD. It is worth noting that for KICH, KIRC, KIRP, and THCA, *NOL7* expression was markedly downregulated during disease progression. However, *NOL7* expression showed no significant change during disease progression in several cancers, including cervical squamous cell carcinoma (CESC), PAAD, skin cutaneous melanoma (SKCM), and uterine corpus endometrial carcinoma (UCEC). Furthermore, *NOL7* protein expression was found to be significantly associated with disease progression in multiple cancers, including breast cancer, ovarian cancer, colon cancer, KIRC, HNSC, and LUAD (Supplementary Figure S3).

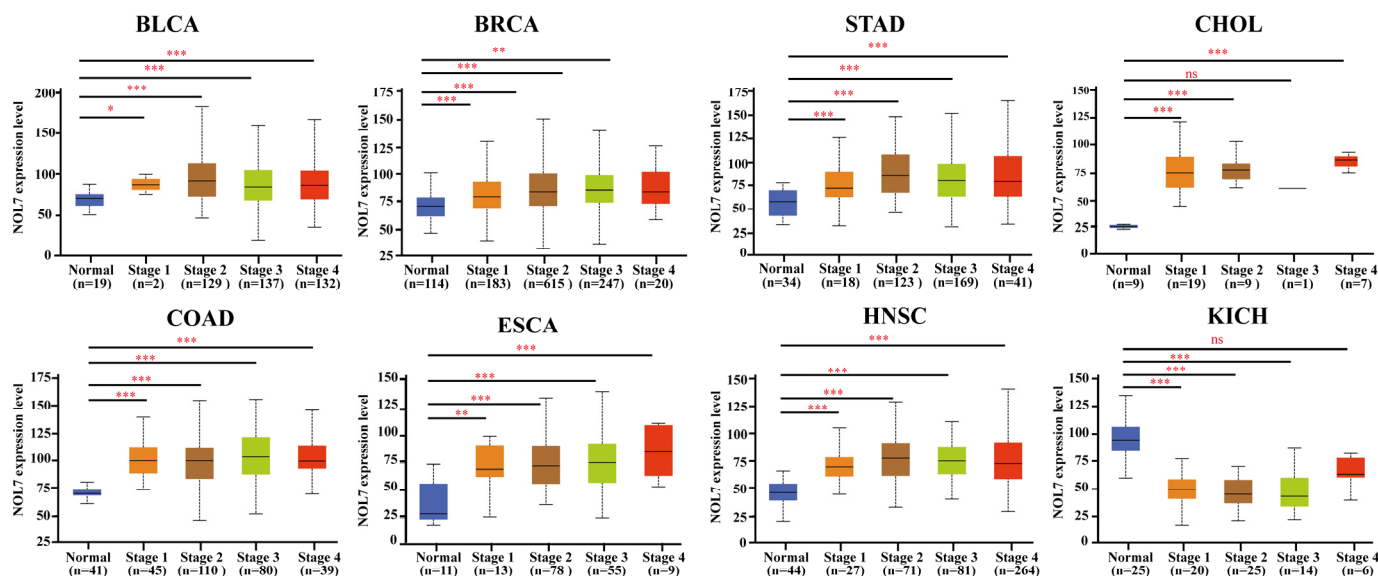


Figure 2. Cont.

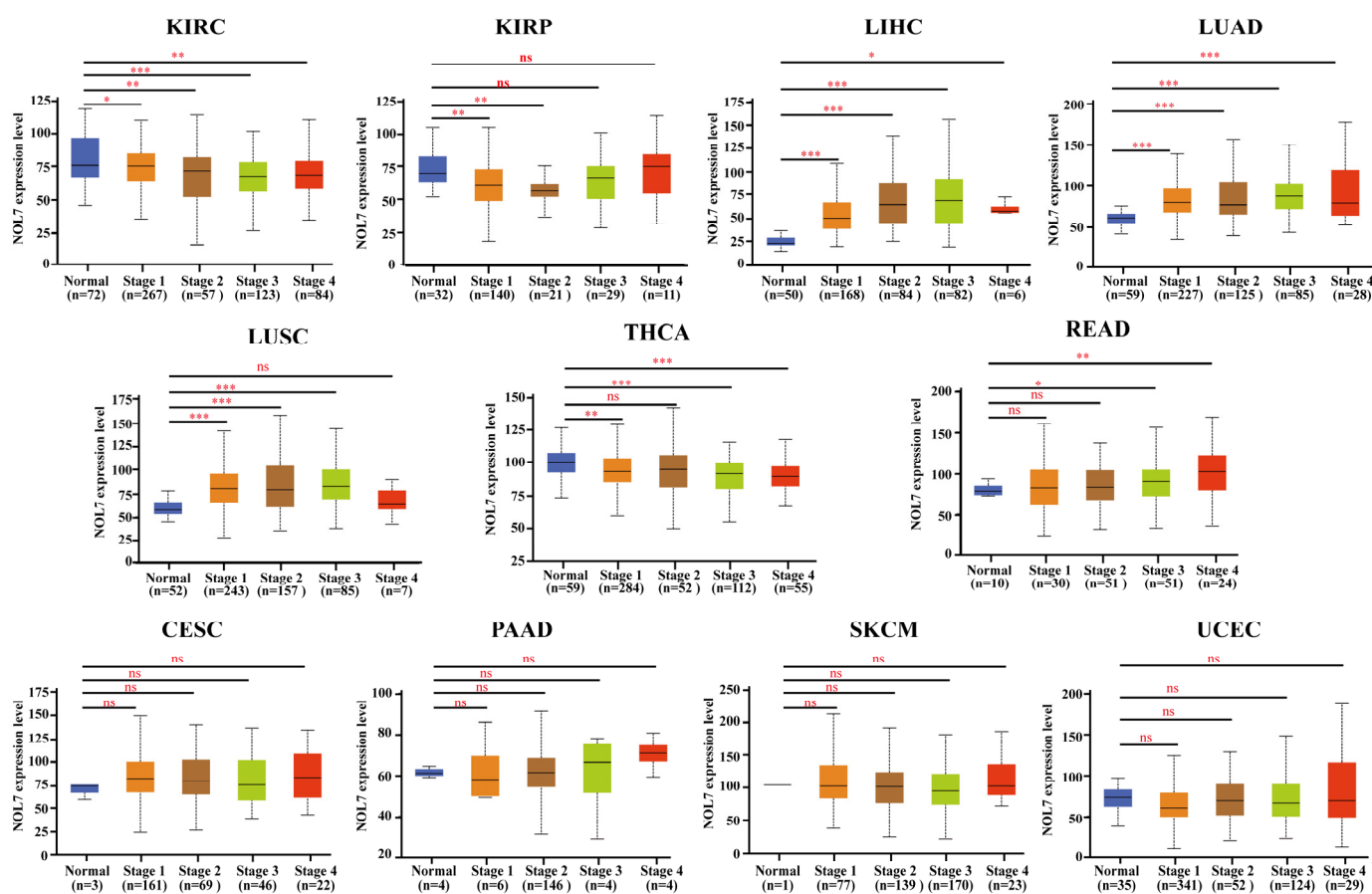
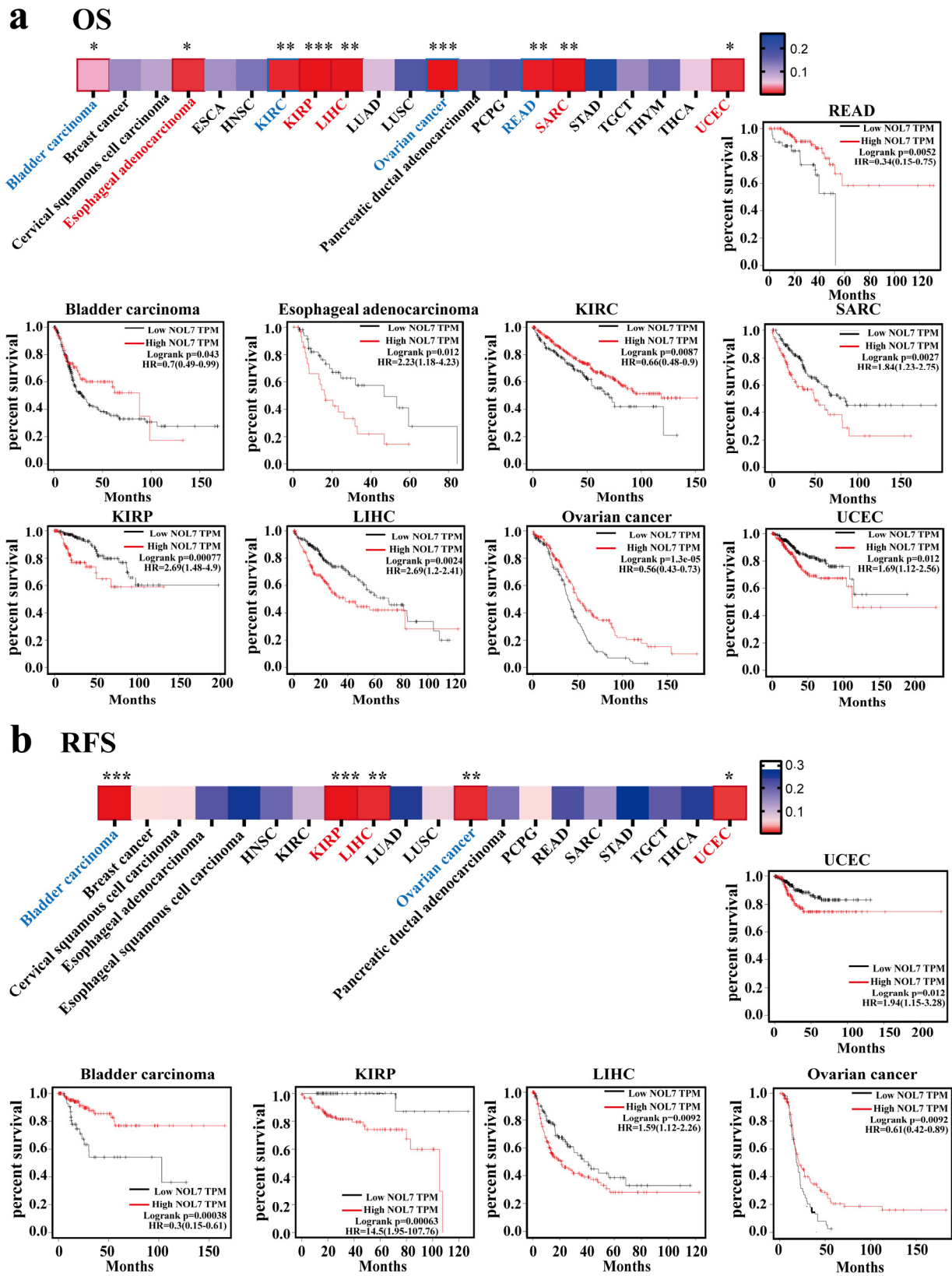


Figure 2. Correlations between *NOL7* gene expression and the main pathological stages in normal and stages I, II, III, and IV BLCA, BRCA, CESC, CHOL, COAD, ESCA, HNSC, KICH, KIRC, KIRP, LIHC, LUAD, LUSC, PAAD, READ, SKCM, STAD, THCA, and UCEC tissues, as examined using the TCGA dataset. * $p < 0.05$; ** $p < 0.01$; *** $p < 0.001$; ns No significance.

2.3. Survival Analysis of *NOL7* in the Pancancer Analysis

To further estimate the correlation between *NOL7* expression and prognosis in human patients with cancers, the Kaplan–Meier plotter and GEPIA2 were utilized, respectively. According to the results from the Kaplan–Meier plotter, Figure 3a suggested that enhanced expression of *NOL7* was associated with poor overall survival (OS) in ESCA ($p < 0.05$), KIRP ($p < 0.001$), LIHC ($p < 0.01$), sarcoma (SARC) ($p < 0.001$), and UCEC ($p < 0.05$). Among all tumor types, KIRP showed the greatest significance. In contrast, reduced *NOL7* expression was related to favorable OS in bladder carcinoma ($p < 0.05$), KIRC ($p < 0.01$), ovarian cancer ($p < 0.001$), and READ ($p < 0.001$). Figure 3b illustrates that highly expressed *NOL7* was negatively correlated with relapse-free survival (RFS) in KIRP, LIHC, and UCEC and positively correlated with RFS in bladder carcinoma ($p < 0.001$) and ovarian cancer ($p < 0.01$). In addition, increased *NOL7* expression corresponded with poor distant metastasis-free survival (DMFS) ($p < 0.05$) and RFS ($p < 0.001$) in breast cancer but was related to better OS ($p < 0.001$), first progression (FP) ($p < 0.001$), and post-progression survival (PPS) ($p < 0.001$) in gastric cancer. Additionally, increased *NOL7* expression was remarkably related to poor PFS ($p < 0.001$) and better PPS ($p < 0.01$) in ovarian cancer and to better FP ($p < 0.001$) in lung cancer (Supplementary Figure S4). Moreover, subgroup analyses of breast cancer, lung cancer, gastric cancer, ovarian cancer, and liver cancer were conducted to investigate the association between *NOL7* expression and the prognoses of patients in the different groups (Supplementary Tables S1–S5).



According to the results from GEPIA2, we observed that dysregulated NOL7 expression significantly affected OS in seven types of cancer. For KIRC and OV, a favorable prognosis was presented when NOL7 expression was increased (all p -values < 0.001); the indications were opposite for other cancers, including ACC, ESCA, KICH, SARC, and LIHC (all p -values < 0.05; Supplementary Figure S5a). Supplementary Figure S5b indicates that highly expressed NOL7 predicted poor DFS for ACC, CHOL, HNSC, LIHC, KICH, SKCM, and uterine carcinosarcoma (UCS) (all p -values < 0.05). However, augmented NOL7 expression predicted a good prognosis in terms of OS in both KIRC and OV (all p -values < 0.05). Taken together, these results demonstrated that NOL7 expression could predict patient survival in several cancer types, especially ACC, KICH, KIRC, LIHC, LUAD, and OV. However, the specific relationship between NOL7 expression level and prognosis in cancer patients depends on the tumor type.

2.4. Pancancer Analysis of DNA Methylation Levels and Genetic Alteration of NOL7

Abnormal DNA methylation was reported to lead to an increased risk of cancer [14]. Based on the TCGA project, we used UALCAN to explore the potential relationship between NOL7 DNA methylation level and tumorigenesis. A significant decrease in the methylation level of NOL7 was observed in HNSC, BLCA, ESCA, LUAD, LUSC, PRAD, pheochromocytoma and paraganglioma (PCPG), testicular germ cell tumors (TGCTs), THCA, UCEC (all p -values < 0.001), KIRP, and ESCA (all p -values < 0.01) as compared with normal tissues (Figure 4a). However, no differences were observed between BRCA, CHOL, COAD, CESC, GBM, KIRC, PAAD, READ, STAD, SARC, and THYM tissues and matching normal tissues (Supplementary Figure S6).

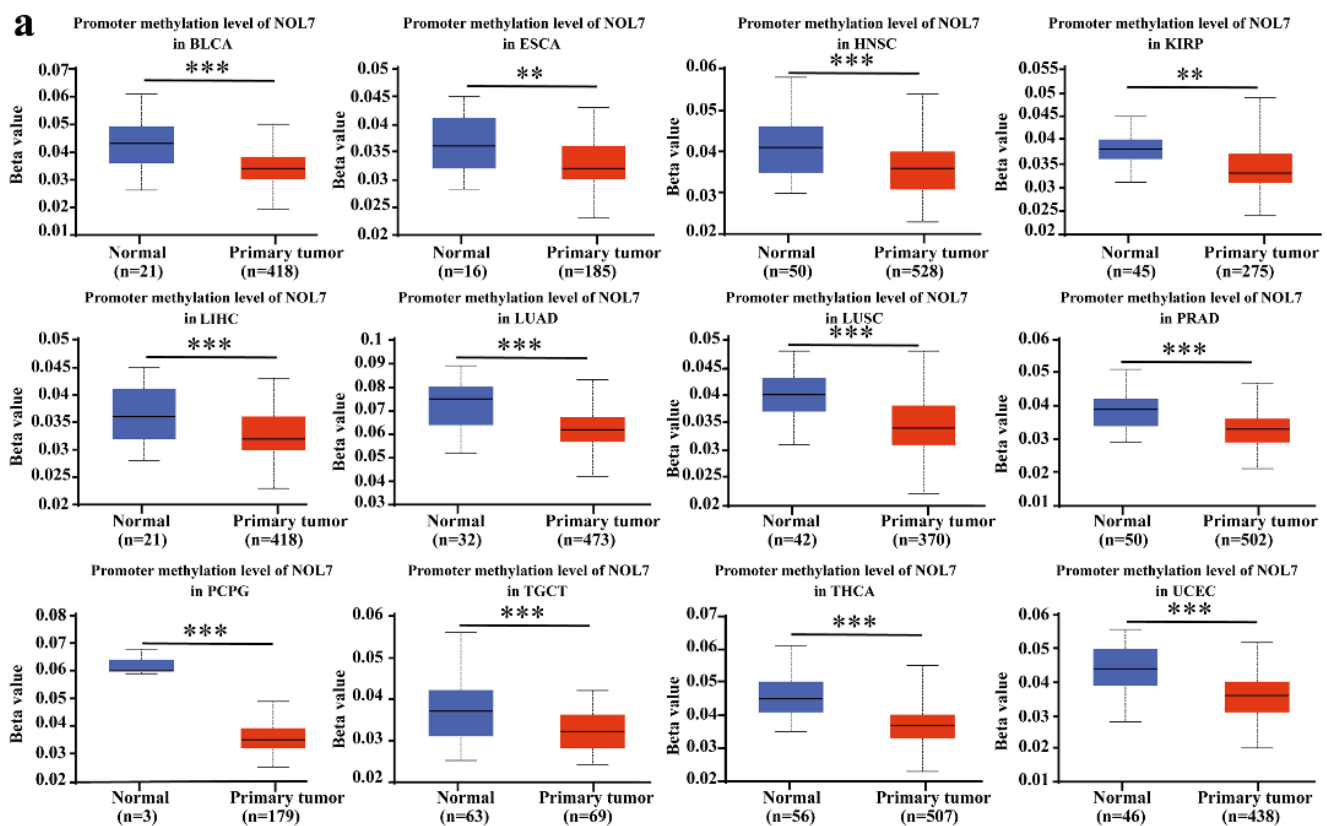


Figure 4. Cont.

the correlation between NOL7 expression and immune infiltration level. As shown in Figure 5, NOL7 expression was significantly correlated with the abundance of infiltrating immune cells: CD4+ T cells in 14 types of cancer, CD8+ T cells in 16 types of cancer, B cells in 11 types of cancer, neutrophils in 16 types of cancer, macrophages in 14 types of cancer, and DCs in 18 types of cancer. Additionally, NOL7 expression was positively and significantly correlated with these immune cells in KIRC, PRAD, KICH, LIHC, OV, and PAAD. CD8+ T cells and neutrophils were most strongly positively associated with NOL7 expression in these different cancers. Moreover, the results of the immune checkpoint analysis showed that NOL7 expression in most tumor tissues was positively correlated with C10orf54, CD276, IL12A, and especially HMGB1. The above results indicate that NOL7 may be a potential target for immune therapy (Supplementary Figure S7).

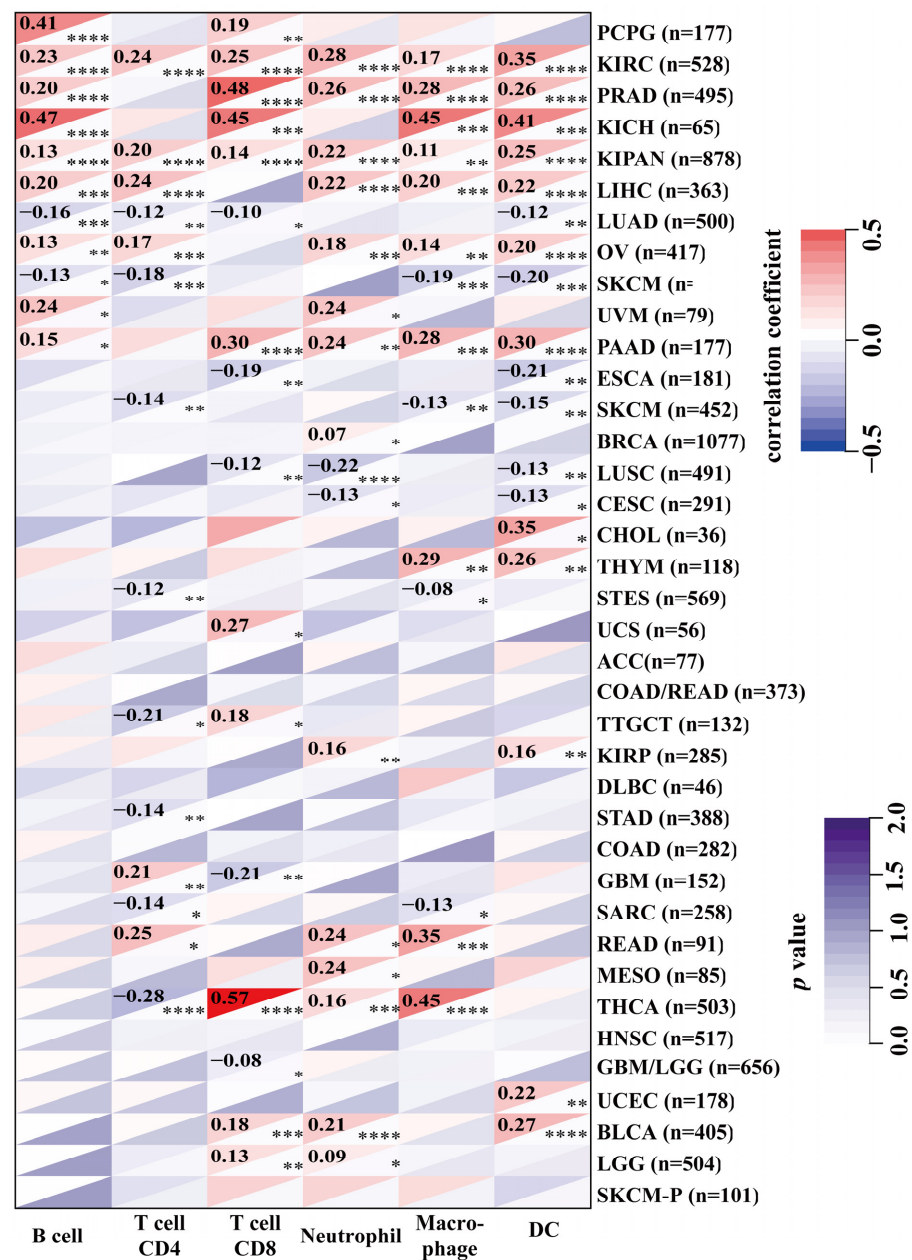


Figure 5. Association between NOL7 expression and immune infiltration levels in various immune cells in the TIMER2.0 database, as assessed using the Sangerbox tool. * $p < 0.05$; ** $p < 0.01$; *** $p < 0.001$; **** $p < 0.0001$.

We further explored the correlations between NOL7 expression and TMB and MSI. A positive correlation between NOL7 expression and MIS was observed in GBM, brain lower-grade glioma (LGG), stomach and esophageal carcinoma (STES), SARC, STAD, UCEC, HNSC, KIRC, LUSC, and UCS. In addition, NOL7 expression was positively correlated with TMB in LUAD, LAML, BRCA, ESCA, STES, SARC, STAD, LUSC, THYM, LIHC, PAAD, SKCM, UCS, BLCA, and ACC (Supplementary Figure S8).

2.6. Gene Enrichment Analysis of NOL7 in the Pancancer Analysis

NOL7-interacting molecules and NOL7-correlated genes were selected to conduct GO and KEGG pathway enrichment analyses. We obtained the top 100 genes related to NOL7 expression in 33 human cancers based on GEPIA2. The top five related genes were MCUR1 (R = 0.6), EEF1E1 (R = 0.61), SSB (R = 0.57), DHX9 (R = 0.53), and WRNIP1 (R = 0.6) (all p-values < 0.01) (Figure 6a, above). The correlation heatmap data showed that the expression of NOL7 was positively correlated with the expression of these genes in the majority of detailed cancer types (Figure 6a, below). In addition, we used the STRING tool to collect the top 50 NOL7-interacting proteins, which identifications were supported by experimental evidence. The PPI network for these 50 proteins is shown in Figure 6b. Moreover, four common members were obtained by intersection analysis of NOL7-interacting and -correlated genes: NIFK, MPHOSPH10, NOL10, and WDR12 (Figure 6c).

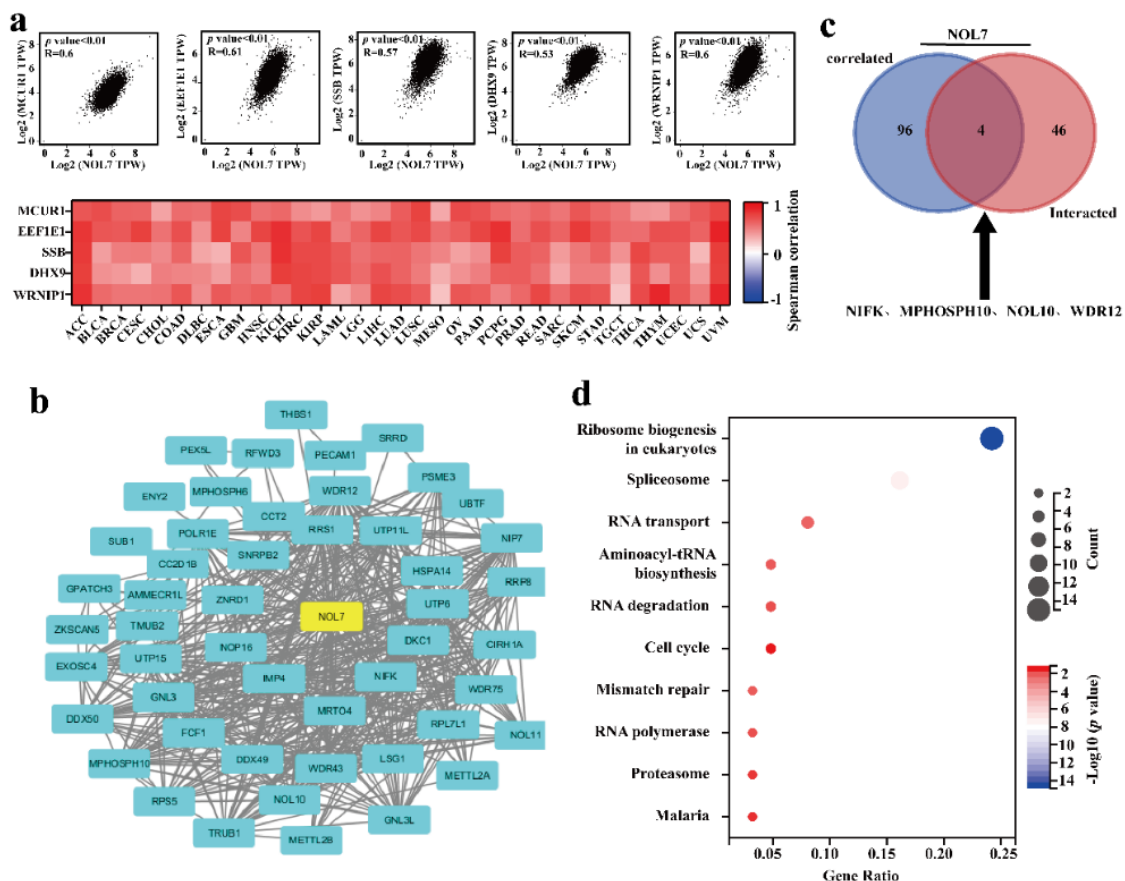


Figure 6. Cont.

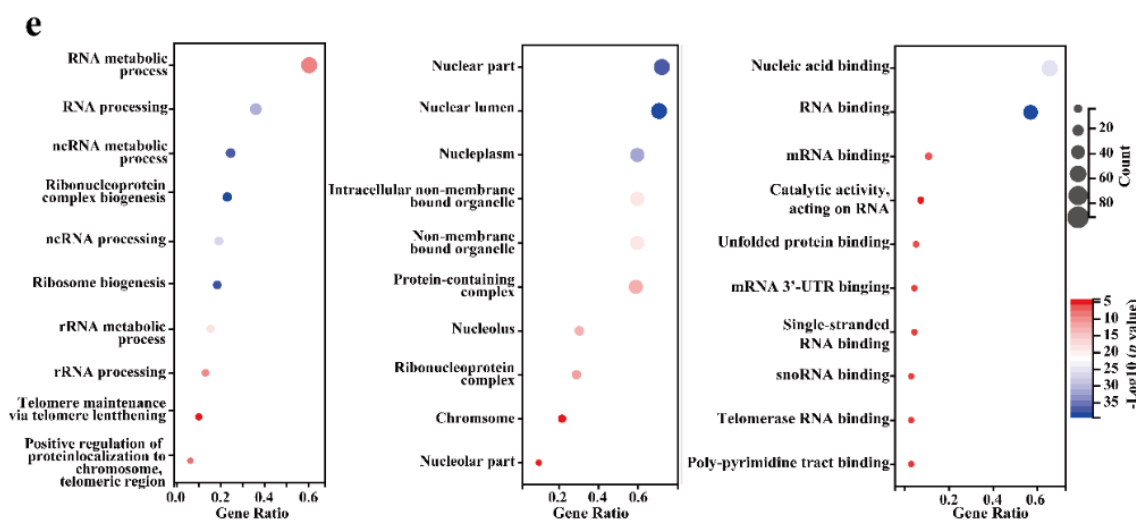


Figure 6. Enrichment analysis of *NOL7*-related genes. (a) The top 100 genes related to *NOL7* expression were obtained from the TCGA project, and the correlations between *NOL7* expression and selected target genes, including *MCUR1*, *EEF1E1*, *SSB*, *DHX9*, *WRNIP1*, and *ABT1*, were analyzed using GEPIA2. (b) A PPI network of 50 experimentally verified *NOL7*-interacting proteins. The corresponding heatmap data for the detailed cancer types are shown below. (c) An intersection analysis of the *NOL7*-interacting and *NOL7*-correlated genes was conducted, and four genes were obtained, including *NIFK*, *MPHOSPH10*, *NOL10*, and *WDR12*. (d) KEGG pathway analysis of *NOL7*-interacting genes and *NOL7*-correlated genes. (e) GO analysis of *NOL7*-interacting genes and *NOL7*-correlated genes. Enrichment results for biological processes (**left**), cellular component (**middle**), and molecular functions (**right**) are displayed.

According to the results of the KEGG pathway analysis, “ribosome biogenesis”, “spliceosome”, and “RNA transport” were mainly involved in the effects of *NOL7* on tumor pathogenesis (Figure 6d). The GO enrichment analysis suggested that most of the *NOL7*-related genes were closely linked to biological processes, such as the RNA metabolic process, RNA processing, and ncRNA metabolic processes (Figure 6e). These results highlighted the central role of *NOL7* in intracellular molecule synthesis and cell proliferation.

3. Discussion

Existing studies have suggested the tumor-suppressive activity of *NOL7* in cervical cancer [5]. Our previous research first proposed an oncogenic role for *NOL7* in melanoma tumorigenesis and metastasis [13]. Based on the expected function of *NOL7* in human cancer, we conducted a pancancer analysis to characterize the expression landscape of *NOL7* in various cancer types and further explore its prognostic value, genetic alterations, correlation with the cancer immune microenvironment, and regulatory network, aiming to better understand the potential features of *NOL7* in human cancers.

Our study identified the aberrant expression (typically overexpression) of the *NOL7* gene in more than half of all cancer types (33 assessed in total) compared with normal tissues. Integration of these data with CPTAC datasets revealed that both gene and protein expression levels of *NOL7* were significantly enhanced in breast cancer, colon cancer, hepatocellular carcinoma, LUAD, and HNSC. Consistently, both gene and protein expression of *NOL7* were upregulated, along with disease progression in various cancers, including colon cancer, LUAD, and HNSC (Figures 1 and 2 and Supplementary Figure S3). These results suggested that *NOL7* may be pro-carcinogenic and function as a promising diagnostic biomarker for these cancers. It is notable that a potential contradictory of *NOL7* expression was observed in several cancers. For instance, the gene expression level of *NOL7* was found to be upregulated in PAAD, whereas its protein expression level was downregulated. The gene expression level of *NOL7* was decreased, along with disease progression in KIRC, but

its protein expression level was increased (Figures 1 and 2 and Supplementary Figure S3). It is well established that genes do not act in isolation: the expression of gene-coded proteins is affected by many factors, including other genes, the environment, and epigenetics [16]. Crucially, mRNA transcription does not necessarily translate into protein expression, and it is not uncommon to observe a discrepancy between mRNA and protein expression [17]. Inconsistent expression at the gene level and at the protein level for *NOL7* in the same cancer type implies that the mechanisms of *NOL7* expression regulation are well worth exploring. The specific function of *NOL7* in different cancers depends on the particular cancer type, and gain- and loss-of-function approaches will hopefully be able to verify its exact functions. Furthermore, together with the results of the survival analysis performed with both the Kaplan–Meier plotter and GEPIA2, these results indicated the prognostic value of *NOL7* in various cancer types. Among them, highly expressed *NOL7* predicted unfavorable OS, RFS, and DFS in LIHC, whereas it predicted favorable OS, RFS, and DFS in OV. These results illustrated the meaningful prognostic value of *NOL7* with respect to survival in LIHC and OV (Figure 3 and Supplementary Figures S4 and S5). Based on these observations, the critical function of *NOL7* in LIHC can be recognized, with the implication of oncogenic activities of *NOL7* in the carcinogenesis and cancer development of LIHC and the relevance of *NOL7* to patient survival.

Previous researchers have confirmed that consistent loss of *NOL7* through loss of heterozygosity and decreased mRNA and protein expression has been observed in cervical cancer [7]. Additionally, the experimental study performed by Lingen MW et al. also confirmed the suppressive function of *NOL7* in cervical cancer [7]. However, the chromosome region 6p21–23, where *NOL7* resides, is frequently amplified in several cancers, including melanoma, and therefore may exert disease-promoting effects in these cancers [12]. In this study, significantly increased *NOL7* expression was found in metastatic sites as compared with primary sites in SKCM, suggesting the promotion of melanoma development. These findings were consistent with our previous conclusion [13], whereas gain in chromosome 6p21–23 is not frequently reported in hepatocellular carcinoma; thus, whether *NOL7* promotes carcinogenesis in hepatocellular carcinoma awaits verification [18].

Meanwhile, it was pointed out that nucleolus-localized *NOL7* protein is required to maintain internal nucleolar structure and cell proliferation [11]. This implies that the *NOL7*-encoding protein is an essential molecule for cytogenetic events and that loss of *NOL7* leads to the fatal destruction of cancer cells with uncontrollable proliferation properties. In addition, it has been reported that *NOL7* functions as an mRNA-binding protein [9,10]. GO enrichment analysis results also supported the previous findings and reflected a clearer and more exhaustive role for *NOL7* with respect to RNA, for instance, in RNA metabolic process and RNA processing. More importantly, KEGG pathway analysis results revealed that *NOL7*-related genes were mainly involved in ribosome biogenesis. Four genes that closely interacted with *NOL7* (*NIFK*, *MPHOSPH10*, *NOL10*, and *WDR12*) which were identified in our study were implicated in ribosome biogenesis (Figure 6). Ribosomes are responsible for protein synthesis in living cells. The essential roles of increased ribosome biogenesis and protein synthesis in sustaining tumor growth and progression are well established [19], and although a correlation between *NOL7* and ribosome biogenesis has not been reported, it is indicated that *NOL7* expression is strongly correlated with ribosome biogenesis. Furthermore, this relationship could be connected to *NOL7*'s tumor-promoting function. This finding suggested a novel regulatory mechanism for *NOL7* in cancer that deserves further investigation. Our study congruously supported these feasible molecular mechanisms.

DNA methylation is a major epigenetic event that regulates gene expression without modifying DNA sequences [20]. The suppression or inactivation of tumor suppressor genes caused by the hypermethylation of DNA promoter regions is commonly reported in cancer cells [21]. Here, we have shown that the DNA methylation level of *NOL7* was downregulated in most types of cancer, which is consistent with the upregulation of *NOL7* (Figure 4 and Supplementary Figure S6). Furthermore, the tumor immune microenvironment (TME)

is a complex structure consisting of immune cells, endothelial cells, fibroblasts, and other substances. Interaction between cancer cells and various components of the TME favors the immune escape of tumors and eventually leads to the activated proliferation and invasion of cancer cells, which processes are related to tumor recurrence and the survival of patients [22,23]. The present study revealed that *NOL7* expression was significantly correlated with the infiltration levels of several types of immune cells, including B cells, CD8+ T cells, CD4+ T cells, macrophages, neutrophils, and DCs, in many cancers (Figure 6). This study also analyzed the relationship between *NOL7* expression and the expression of 60 common immune checkpoint genes, and notably found that *NOL7* expression was positively correlated with HMGB1 in most cancer types (Supplementary Figure S7). HMGB1 encodes high mobility group box 1, which is a multifunctional molecule that participates in a variety of cellular biological properties, including DNA damage repair and maintenance of genomic stability, and is further involved in the regulation of the inflammatory response and the TME [24]. Our study suggests that *NOL7* might interact with HMGB1, thus functioning as a key mediator related to prognosis and the status of tumor immunity in cancers.

4. Materials and Methods

4.1. Gene Expression Analysis

The expression data for *NOL7* in different normal cells and tissues were downloaded from the HPA database directly. The sample source and ethical statement were provided at <https://www.proteinatlas.org/> (accessed on 19 June 2022) [25]. Low specificity was defined by normalized expression (NX) ≥ 1 in at least one tissue/region/cell type but not elevated in any tissue/region/cell type. The expression differences between normal and tumor tissues in the TCGA database were assessed using TIMER2.0 (<http://timer.cistrome.org/>, accessed on 19 June 2022), based on the TCGA project [26,27].

Since several tumor tissues assessed with TIMER2.0 did not include adjacent normal tissues, we combined the data from the TCGA database with GTEx data for supplementary analyses of the expression differences between normal and tumor tissues through GEPIA2 (<http://gepia2.cancer-pku.cn/>, accessed on 19 June 2022) [28]. We selected the available tumor datasets, including LAML, THYM, CHOL, DLBC, LIHC, and PAAD, based on the significant differences in expression between tumor tissues and normal tissues. In addition, through the visualization of the CPTAC dataset via the UALCAN tool (<http://ualcan.path.uab.edu/analysis-prot.html>, accessed on 21 June 2022), we obtained the differences in total protein expression levels of *NOL7* between adjacent normal tissues and tumor tissues [29]. Furthermore, to explore the relationship between the expression of *NOL7* and tumor staging, we conducted a survey on UALCAN.

4.2. Survival Prognosis Analysis

The OS, RFS, FP, PFS, PPS, DMFS, and DSS of all tumor patients in the GEO cohorts were analyzed using the Kaplan–Meier plotter tool (<http://kmplot.com/analysis/>, accessed on 24 June 2022) [30]. By setting the parameter to “auto select best cutoff”, patients were divided into two groups. Kaplan–Meier survival curves were obtained, and the log-rank *p*-values and HRs were calculated. Moreover, we analyzed the OS and DFS of all tumors using the “survival analysis” module of GEPIA2 (<http://gepia.cancer-pku.cn/index.html>, accessed on 19 June 2022) by setting the group cutoff to “median”. Patients were divided into a high group and a low group to generate Kaplan–Meier survival curves and survival maps and to calculate the log-rank *p*-values and HRs.

4.3. DNA Methylation Analysis and Genetic Alteration Analysis

The UALCAN tool was used to explore the DNA methylation levels for *NOL7* between the various cancer tissues as compared with normal tissues. In addition, we chose the “TCGA Pan-Cancer Atlas Studies” module in the cBioPortal tool (<https://www.cbioportal.org/>, accessed on 1 July 2022) to analyze the genetic variation in *NOL7* [31]. Alteration

frequency, mutation site, and survival data were downloaded by choosing “cancer types summary”, “mutations”, and “comparison/survival” in the query module.

4.4. Immune Infiltration Analysis

We used the Sangerbox tool (<http://sangerbox.com/>, accessed on 17 June 2022) to explore the association between *NOL7* expression and immune infiltration across 33 types of tumors by choosing the “immune cell analysis (TIMER)” module. In addition, the association between *NOL7* expression and many immune-checkpoint-related proteins was assessed by choosing the “immune checkpoint gene analysis” module in the same tool. Furthermore, we examined the relationship between *NOL7* expression and TMB or MSI in different tumors in the TCGA cohort [32]. Spearman’s correlation test was used to calculate *p*-values and partial correlation values.

4.5. Gene Enrichment Analysis

To explore the regulatory network of *NOL7* in cancers, the STRING tool (<https://cn.string-db.org/>, accessed on 21 June 2022) was used to download the top 50 *NOL7*-interacting molecules. We visualized the PPI network using Cytoscape [33]. In addition, we obtained the top 100 *NOL7*-correlated genes through GEPIA2. Pearson’s correlation test was performed on the top five *NOL7*-correlated genes in the “correlation analysis” module of GEPIA2 to obtain *p*-values, dot plots, a heatmap, and correlation coefficients. Moreover, we generated a Venn diagram, combining the two parts using the Draw Venn Diagram tool (<http://bioinformatics.psb.ugent.be/webtools/Venn/>, accessed on 21 June 2022) [34]. We combined these two sets of data and performed a GO enrichment analysis and a KEGG pathway analysis using the R package “cluster profile” in R software. A *p*-value < 0.05 and an FDR < 0.25 were considered statistically significant.

5. Conclusions

Overall, our first pancancer study enabled a relatively comprehensive understanding of the potential role of *NOL7* in various human cancers. We propose that *NOL7* may serve as a new diagnostic biomarker and therapeutic target in different tumor types, including breast cancer, colon cancer, lung cancer, and liver cancer. In addition, our work expands the understanding of the impact of *NOL7* on cancer immunologic therapy, as we revealed strong correlations between *NOL7* and immune cells and immune checkpoints. Future experimental and prospective studies of *NOL7* in different cancer types may provide in-depth insights into regulatory mechanisms and further support the development of therapeutic strategies targeting *NOL7*.

Supplementary Materials: The following supporting information can be downloaded at: <https://www.mdpi.com/article/10.3390/ijms23179611/s1>.

Author Contributions: Y.L. conceived and designed the project. Y.L. and Q.L. performed the surveys. R.X. and Y.L. wrote and revised the manuscript. All authors have read and agreed to the published version of the manuscript.

Funding: This research was funded by the doctoral startup fund of Gannan Medical University QD202132 (Yumei Li) and QD202136 (Renjian Xie).

Institutional Review Board Statement: Not applicable.

Informed Consent Statement: Not applicable.

Data Availability Statement: Please contact the author regarding data requests.

Conflicts of Interest: The authors declare no conflict of interest.

References

1. Feng, Q.; Bian, X.; Liu, X.; Wang, Y.; Zhou, H.; Ma, X.; Quan, C.; Yao, Y.; Zheng, Z. Intracellular expression of arginine deiminase activates the mitochondrial apoptosis pathway by inhibiting cytosolic ferritin and inducing chromatin autophagy. *BMC Cancer* **2020**, *20*, 665. [[CrossRef](#)] [[PubMed](#)]
2. Zhang, X.; Wang, F.; Wang, Z.; Yang, X.; Yu, H.; Si, S.; Lu, J.; Zhou, Z.; Lu, Q.; Wang, Z.; et al. ALKBH5 promotes the proliferation of renal cell carcinoma by regulating AURKB expression in an mA-dependent manner. *Ann. Transl. Med.* **2020**, *8*, 646. [[CrossRef](#)] [[PubMed](#)]
3. Chen, Y.; Zhao, H.; Xiao, Y.; Shen, P.; Tan, L.; Zhang, S.; Liu, Q.; Gao, Z.; Zhao, J.; Zhao, Y.; et al. Pan-cancer analysis reveals an immunological role and prognostic potential of PXN in human cancer. *Aging* **2021**, *13*, 16248–16266. [[CrossRef](#)] [[PubMed](#)]
4. Mankame, T.P.; Zhou, G.; Lingen, M.W. Identification and characterization of the human NOL7 gene promoter. *Gene* **2010**, *456*, 36–44. [[CrossRef](#)] [[PubMed](#)]
5. Hasina, R.; Pontier, A.L.; Fekete, M.J.; Martin, L.E.; Qi, X.M.; Brigaudeau, C.; Pramanik, R.; Cline, E.I.; Coignet, L.J.; Lingen, M.W. NOL7 is a nucleolar candidate tumor suppressor gene in cervical cancer that modulates the angiogenic phenotype. *Oncogene* **2006**, *25*, 588–598. [[CrossRef](#)]
6. Huang, L.; Zheng, M.; Zhou, Q.-M.; Zhang, M.-Y.; Yu, Y.-H.; Yun, J.-P.; Wang, H.-Y. Identification of a 7-gene signature that predicts relapse and survival for early stage patients with cervical carcinoma. *Med. Oncol.* **2012**, *29*, 2911–2918. [[CrossRef](#)]
7. Doçi, C.L.; Mankame, T.P.; Langerman, A.; Ostler, K.R.; Kanteti, R.; Best, T.; Onel, K.; Godley, L.A.; Salgia, R.; Lingen, M.W. Characterization of NOL7 gene point mutations, promoter methylation, and protein expression in cervical cancer. *Int. J. Gynecol. Pathol.* **2012**, *31*, 15–24. [[CrossRef](#)]
8. Mankame, T.P.; Lingen, M.W. The RB tumor suppressor positively regulates transcription of the anti-angiogenic protein NOL7. *Neoplasia* **2012**, *14*, 1213–1222. [[CrossRef](#)]
9. Doçi, C.L.; Zhou, G.; Lingen, M.W. The novel tumor suppressor NOL7 post-transcriptionally regulates thrombospondin-1 expression. *Oncogene* **2013**, *32*, 4377–4386. [[CrossRef](#)]
10. Zhou, G.; Doçi, C.L.; Lingen, M.W. Identification and functional analysis of NOL7 nuclear and nucleolar localization signals. *BMC Cell Biol.* **2010**, *11*, 74. [[CrossRef](#)]
11. Kinor, N.; Shav-Tal, Y. The dynamics of the alternatively spliced NOL7 gene products and role in nucleolar architecture. *Nucleus* **2011**, *2*, 229–245. [[CrossRef](#)] [[PubMed](#)]
12. Santos, G.C.; Zielenska, M.; Prasad, M.; Squire, J.A. Chromosome 6p amplification and cancer progression. *J. Clin. Pathol.* **2007**, *60*, 1–7. [[CrossRef](#)] [[PubMed](#)]
13. Li, Y.; Zhong, C.; Wang, J.; Chen, F.; Shen, W.; Li, B.; Zheng, N.; Lu, Y.; Katanaev, V.L.; Jia, L. NOL7 facilitates melanoma progression and metastasis. *Signal Transduct. Target. Ther.* **2021**, *6*, 352. [[CrossRef](#)] [[PubMed](#)]
14. Patai, A.V.; Molnár, B.; Kalmár, A.; Schöller, A.; Tóth, K.; Tulassay, Z. Role of DNA methylation in colorectal carcinogenesis. *Dig. Dis.* **2012**, *30*, 310–315. [[CrossRef](#)]
15. Sun, J.; Zhang, Z.; Bao, S.; Yan, C.; Hou, P.; Wu, N.; Su, J.; Xu, L.; Zhou, M. Identification of tumor immune infiltration-associated lncRNAs for improving prognosis and immunotherapy response of patients with non-small cell lung cancer. *J. Immunother. Cancer* **2020**, *8*. [[CrossRef](#)]
16. de Andrade, M.; Warwick Daw, E.; Kraja, A.T.; Fisher, V.; Wang, L.; Hu, K.; Li, J.; Romanescu, R.; Veenstra, J.; Sun, R.; et al. The challenge of detecting genotype-by-methylation interaction: GAW20. *BMC Genet.* **2018**, *19* (Suppl. 1), 81. [[CrossRef](#)]
17. O’Leary, P.C.; Penny, S.A.; Dolan, R.T.; Kelly, C.M.; Madden, S.F.; Rexhepaj, E.; Brennan, D.J.; McCann, A.H.; Pontén, F.; Uhlén, M.; et al. Systematic antibody generation and validation via tissue microarray technology leading to identification of a novel protein prognostic panel in breast cancer. *BMC Cancer* **2013**, *13*, 175. [[CrossRef](#)]
18. Furge, K.A.; Dykema, K.J.; Ho, C.; Chen, X. Comparison of array-based comparative genomic hybridization with gene expression-based regional expression biases to identify genetic abnormalities in hepatocellular carcinoma. *BMC Genom.* **2005**, *6*, 67. [[CrossRef](#)]
19. Pelletier, J.; Thomas, G.; Volarević, S. Ribosome biogenesis in cancer: New players and therapeutic avenues. *Nat. Rev. Cancer* **2018**, *18*, 51–63. [[CrossRef](#)]
20. Mehdi, A.; Rabbani, S.A. Role of Methylation in Pro- and Anti-Cancer Immunity. *Cancers* **2021**, *13*, 545. [[CrossRef](#)]
21. Wang, M.; Ngo, V.; Wang, W. Deciphering the genetic code of DNA methylation. *Brief Bioinform.* **2021**, *22*, bbaa424. [[CrossRef](#)] [[PubMed](#)]
22. Ohtani, H. Focus on TILs: Prognostic significance of tumor infiltrating lymphocytes in human colorectal cancer. *Cancer Immun.* **2007**, *7*, 4.
23. Yoshihara, K.; Shahmoradgoli, M.; Martínez, E.; Vegesna, R.; Kim, H.; Torres-Garcia, W.; Treviño, V.; Shen, H.; Laird, P.W.; Levine, D.A.; et al. Inferring tumour purity and stromal and immune cell admixture from expression data. *Nat. Commun.* **2013**, *4*, 2612. [[CrossRef](#)] [[PubMed](#)]
24. Wang, S.; Zhang, Y. HMGB1 in inflammation and cancer. *J. Hematol. Oncol.* **2020**, *13*, 116. [[CrossRef](#)] [[PubMed](#)]
25. Uhlén, M.; Fagerberg, L.; Hallström, B.M.; Lindskog, C.; Oksvold, P.; Mardinoglu, A.; Sivertsson, Å.; Kampf, C.; Sjöstedt, E.; Asplund, A.; et al. Proteomics. Tissue-based map of the human proteome. *Science* **2015**, *347*, 1260419. [[CrossRef](#)] [[PubMed](#)]
26. Li, T.; Fu, J.; Zeng, Z.; Cohen, D.; Li, J.; Chen, Q.; Li, B.; Liu, X.S. TIMER2. 0 for analysis of tumor-infiltrating immune cells. *Nucleic Acids Res.* **2020**, *48*, W509–W514. [[CrossRef](#)]

27. Li, T.; Fan, J.; Wang, B.; Traugh, N.; Chen, Q.; Liu, J.S.; Li, B.; Liu, X.S. TIMER: A web server for comprehensive analysis of tumor-infiltrating immune cells. *Cancer Res.* **2017**, *77*, e108–e110. [[CrossRef](#)]
28. Tang, Z.; Kang, B.; Li, C.; Chen, T.; Zhang, Z. GEPIA2: An enhanced web server for large-scale expression profiling and interactive analysis. *Nucleic Acids Res.* **2019**, *47*, W556–W560. [[CrossRef](#)]
29. Chandrashekar, D.S.; Bashel, B.; Balasubramanya, S.A.H.; Creighton, C.J.; Ponce-Rodriguez, I.; Chakravarthi, B.V.S.K.; Varambally, S. UALCAN: A Portal for Facilitating Tumor Subgroup Gene Expression and Survival Analyses. *Neoplasia* **2017**, *19*, 649–658. [[CrossRef](#)] [[PubMed](#)]
30. Lánckzy, A.; Győrffy, B. Web-based survival analysis tool tailored for medical research (KMplot): Development and implementation. *J. Med. Internet Res.* **2021**, *23*, e27633. [[CrossRef](#)]
31. Gao, J.; Aksoy, B.A.; Dogrusoz, U.; Dresdner, G.; Gross, B.; Sumer, S.O.; Sun, Y.; Jacobsen, A.; Sinha, R.; Larsson, E.; et al. Integrative analysis of complex cancer genomics and clinical profiles using the cBioPortal. *Sci. Signal* **2013**, *6*, p11. [[CrossRef](#)] [[PubMed](#)]
32. Bonneville, R.; Krook, M.A.; Kautto, E.A.; Miya, J.; Wing, M.R.; Chen, H.-Z.; Reeser, J.W.; Yu, L.; Roychowdhury, S. Landscape of Microsatellite Instability Across 39 Cancer Types. *JCO Precis. Oncol.* **2017**, 2017. [[CrossRef](#)] [[PubMed](#)]
33. Shannon, P.; Markiel, A.; Ozier, O.; Baliga, N.S.; Wang, J.T.; Ramage, D.; Amin, N.; Schwikowski, B.; Ideker, T. Cytoscape: A software environment for integrated models of biomolecular interaction networks. *Genome Res.* **2003**, *13*, 2498–2504. [[CrossRef](#)] [[PubMed](#)]
34. Bardou, P.; Mariette, J.; Escudié, F.; Djemiel, C.; Klopp, C. jvenn: An interactive Venn diagram viewer. *BMC Bioinform.* **2014**, *15*, 293. [[CrossRef](#)] [[PubMed](#)]